Inhibition of RNA lariat debranching enzyme suppresses TDP-43 toxicity in ALS disease models

Maria Armakola[1,2,12], Matthew J Higgins[3,12], Matthew D Figley[1], Sami J Barmada[4,5], Emily A Scarborough[6], Zamia Diaz[6], Xiaodong Fang[1], James Shorter[6], Nevan J Krogan[3,7,8], Steven Finkbeiner[4,5,9], Robert V Farese Jr[3,10,11,13] & Aaron D Gitler[1,13]

Amyotrophic lateral sclerosis (ALS) is a devastating neurodegenerative disease primarily affecting motor neurons. Mutations in the gene encoding TDP-43 cause some forms of the disease, and cytoplasmic TDP-43 aggregates accumulate in degenerating neurons of most individuals with ALS. Thus, strategies aimed at targeting the toxicity of cytoplasmic TDP-43 aggregates may be effective. Here, we report results from two genome-wide loss-of-function TDP-43 toxicity suppressor screens in yeast. The strongest suppressor of TDP-43 toxicity was deletion of *DBR1*, which encodes an RNA lariat debranching enzyme. We show that, in the absence of Dbr1 enzymatic activity, intronic lariats accumulate in the cytoplasm and likely act as decoys to sequester TDP-43, preventing it from interfering with essential cellular RNAs and RNA-binding proteins. Knockdown of Dbr1 in a human neuronal cell line or in primary rat neurons is also sufficient to rescue TDP-43 toxicity. Our findings provide insight into TDP-43–mediated cytotoxicity and suggest that decreasing Dbr1 activity could be a potential therapeutic approach for ALS.

ALS, also known as Lou Gehrig's disease, is a late-onset neurodegenerative disease characterized by loss of motor neurons, progressive weakness and eventual paralysis and death within 3–5 years of diagnosis[1]. Most ALS cases are sporadic (SALS), but 10% are familial (FALS), of which ~20% result from mutations in the *SOD1* gene (encoding Cu/Zn superoxide dismutase 1)[2]. *SOD1* mutations are thought to cause disease by a toxic gain of function[3], and, thus, strategies to lower SOD1 levels are being pursued[4]. However, *SOD1* mutations account for only a small percentage of ALS cases, and additional therapeutic strategies are needed.

RNA-binding proteins and RNA-processing pathways have recently been implicated in ALS[5,6]. The RNA-binding protein TDP-43 has been found in cytoplasmic inclusions in the spinal cord neurons of most ALS cases without *SOD1* mutation[7,8], and mutations in *TARDBP*, which encodes TDP-43, have been identified in FALS and SALS cases[9–13]. Mutations in *FUS*, which encodes another RNA-binding protein (FUS, also called TLS), have also been found in some ALS cases[14–18]. Therefore, therapies targeting TDP-43 and/or FUS could be effective in cases not caused by *SOD1* mutation. Notably, TDP-43 inclusions occur in many frontotemporal dementia cases, and targeting TDP-43 might be an effective therapeutic strategy for these patients. Efforts are under way to define the

mechanisms by which TDP-43 and FUS and defects in RNA processing pathways contribute to ALS.

We have used yeast models to illuminate mechanisms underpinning TDP-43 and FUS aggregation and cellular toxicity[19–21]. TDP-43 forms aggregates in the cytoplasm of yeast cells and is toxic, recapitulating two key features of TDP-43 relevant to human disease[19]. We used a genome-wide plasmid overexpression screen to identify modifiers of aggregation and toxicity. One modifier of toxicity was Pbp1, whose human homolog, ataxin 2, harbors a polyglutamine tract that is expanded (>34 glutamines) in spinocerebellar ataxia type 2. We found that intermediate-length polyglutamine expansions (~27–33 glutamines) in ataxin 2 are a genetic risk factor for ALS[22,23]. Additional genetic modifiers of TDP-43 toxicity in yeast might provide further insight into pathogenic mechanisms and could represent novel therapeutic targets.

Here, we report results from a genome-wide loss-of-function screen to identify yeast genes that modify TDP-43 toxicity. In our previous screen (ref. 22 and A.D.G., unpublished data), we used a library of yeast overexpression plasmids. Here, we interrogated collections of nonessential yeast knockouts and knockdowns of essential genes. Loss-of-function screens may be useful to identify therapeutic targets for which inhibitors could be developed. Among the most potent

[1]Department of Genetics, Stanford University School of Medicine, Stanford, California, USA. [2]Neuroscience Graduate Group, Perelman School of Medicine at the University of Pennsylvania, Philadelphia, Pennsylvania, USA. [3]Gladstone Institute of Cardiovascular Disease, J David Gladstone Institutes, San Francisco, California, USA. [4]Gladstone Institute of Neurological Disease, Taube-Koret Center, Hellman Family Foundation Program, J David Gladstone Institutes, San Francisco, California, USA. [5]Department of Neurology, University of California, San Francisco, San Francisco, California, USA. [6]Department of Biochemistry and Biophysics, Perelman School of Medicine at the University of Pennsylvania, Philadelphia, Pennsylvania, USA. [7]Department of Cellular and Molecular Pharmacology, University of California, San Francisco, San Francisco, California, USA. [8]California Institute for Quantitative Biosciences, San Francisco, California, USA. [9]Department of Physiology, University of California, San Francisco, San Francisco, California, USA. [10]Department of Medicine, University of California, San Francisco, San Francisco, California, USA. [11]Department of Biochemistry & Biophysics, University of California, San Francisco, San Francisco, California, USA. [12]These authors contributed equally to this work. [13]These authors jointly directed this work. Correspondence should be addressed to A.D.G. (agitler@stanford.edu) or R.V.F. (bfarese@gladstone.ucsf.edu).

Table 1 Yeast gene deletions that enhance or suppress TDP-43 toxicity

Yeast strain	Effect on TDP-43 toxicity	Function	Human homolog
fld1Δ	Enhancer	Involved in lipid droplet morphology, number and size; proposed to be involved in lipid metabolism	BSCL2 (Berardinelli-Seip congenital lipodystrophy); seipin
mrpl39Δ	Enhancer	Mitochondrial ribosomal protein of the large subunit	MRPL33
msn2Δ	Enhancer	Stress-induced transcriptional activator	None
nhx1Δ	Enhancer	Vacuolar and endosomal Na⁺/H⁺ exchanger involved in pH regulation	SLC9A6
rpl16bΔ	Enhancer	Component of the large (60S) ribosomal subunit	RPL13A
tif4631Δ	Enhancer	Translation initiation factor	EIF4G1
cce1Δ	Suppressor	Mitochondrial cruciform cutting endonuclease, cleaves Holliday junctions formed during recombination of mitochondrial DNA	None
dbr1Δ	Suppressor	RNA lariat debranching enzyme, involved in intron turnover	DBR1
dom34Δ	Suppressor	EndoRNase involved in no-go mRNA decay	PELO
pbp1Δ	Suppressor	Involved in P body–dependent granule assembly; interacts with Pab1p to regulate mRNA polyadenylation	ATXN2
rpl16aΔ	Suppressor	Component of the large (60S) ribosomal subunit	RPL13A
set3Δ	Suppressor	Member of histone deacetylase complex	ASH1
siw14Δ	Suppressor	Tyrosine phosphatase involved in actin filament organization and endocytosis	None
ydr067cΔ	Suppressor	Cytoplasmic protein required for replication of Brome mosaic virus in *S. cerevisiae*, which is a model system for studying replication of positive-stranded RNA viruses in their natural hosts	None

knockout suppressors of TDP-43 toxicity discovered in our screen was *dbr1Δ*. Dbr1 catalyzes the debranching of lariat introns that are formed during pre-mRNA splicing. We show that inhibiting the debranching enzymatic activity of Dbr1 is sufficient to rescue TDP-43 toxicity. We also provide evidence that intronic lariat species that accumulate in the cytoplasm of *dbr1Δ* cells act as decoys to sequester toxic cytoplasmic TDP-43, possibly preventing it from interfering with other essential cellular RNA targets and RNA-binding proteins. Knockdown of Dbr1 in a human neuronal cell line and in primary rat neurons is also sufficient to rescue TDP-43 toxicity, suggesting that the effect of Dbr1 on TDP-43 toxicity is conserved from yeast to mammals. We propose that the debranching enzymatic activity of Dbr1 could be a potential therapeutic target for ALS and related TDP-43 proteinopathies.

RESULTS

DBR1 is a potent modifier of TDP-43 toxicity in yeast

To identify genes that modify TDP-43 toxicity, we performed two independent, unbiased genome-wide yeast deletion screens in two different laboratories (**Supplementary Fig. 1**). Similar approaches have been used to discover modifiers of the neurodegenerative disease proteins α-synuclein, huntingtin and FUS[21,24,25]. In the first screen, we used synthetic genetic array (SGA) analysis[26] to introduce a galactose-inducible plasmid expressing TDP-43 into each nonessential yeast deletion strain by mating (**Supplementary Fig. 1a**). The second screen included the deletion genes and a library of essential genes generated by decreased abundance by mRNA perturbation (DAmP) technology[27] (**Supplementary Fig. 1b–e**). We selected yeast deletion strains in which TDP-43 was more (enhancer) or less (suppressor) toxic than in wild-type cells. Screen 1 was repeated three independent times, and only gene deletions that were reproduced all three times were selected. Screen 2 contained three biological and two technical replicates (six replicates in total), which allowed the calculation of an interaction score (a quantitative assessment of the effectiveness of suppression or enhancement of TDP-43 toxicity). To provide independent evidence that the gene deletions identified from the screens modify TDP-43 toxicity, we generated gene deletions for the hits from screen 1 and selected genes from screen 2 in an independent strain background, confirming the effects on TDP-43 toxicity. In screen 1, we identified 14 yeast deletion strains that modified TDP-43 toxicity (**Table 1**): 6 enhancers

and 8 suppressors. The more sensitive and quantitative analysis in screen 2 allowed us to identify a total of 2,581 potential enhancers and 2,056 potential suppressors (**Supplementary Data**). In analyzing these results, we chose to focus on suppressors of TDP-43 toxicity because these could represent attractive therapeutic targets for small molecule inhibitors or RNA interference (see the **Supplementary Note** for discussion of additional yeast TDP-43 toxicity modifier genes).

One of the most effective deletion suppressors of TDP-43 toxicity identified independently in both screens was *dbr1Δ*, and we focused further efforts on the *DBR1* gene. *DBR1* deletion suppressed the toxicity of wild-type TDP-43, as well as that of an ALS-linked mutant form of TDP-43 (Gln331Lys; **Fig. 1a** and **Supplementary Fig. 2**). Immunoblotting confirmed that toxicity was not suppressed because of lower TDP-43 expression in the *dbr1Δ* strain (**Fig. 1b**). Deletion of *DBR1* did not suppress the toxicity of two other neurodegenerative disease proteins, α-synuclein and mutant huntingtin. Indeed, α-synuclein toxicity was slightly enhanced in the *dbr1Δ* strain (**Fig. 1a**). However, *DBR1* deletion suppressed toxicity of another RNA-binding protein linked to ALS, FUS (**Fig. 1a**), showing specificity of the *DBR1* genetic interaction for ALS-linked RNA-binding proteins TDP-43 and FUS.

Inhibiting DBR1 suppresses TDP-43 toxicity in mammalian cells

Identification of *Dbr1* as a potent modifier of TDP-43 toxicity suggests the possibility that inhibiting Dbr1 enzymatic activity (**Fig. 1c**) could be a promising therapeutic strategy for ALS, especially as TDP-43 is thought to contribute broadly to almost all ALS cases without *SOD1* mutation[7]. Therefore, we tested whether inhibiting Dbr1 function could rescue TDP-43 toxicity in mammalian cells. We generated a stable human M17 neuroblastoma cell line that inducibly expresses epitope-tagged ALS-linked mutant TDP-43 (Gln331Lys) under the control of a doxycycline-regulated promoter (**Fig. 2a**). Inducible expression of TDP-43 Gln331Lys was confirmed by immunofluorescence and immunoblotting (**Fig. 2b** and data not shown). Upregulating mutant TDP-43 was toxic in these cells (**Fig. 2c**). To determine whether inhibiting Dbr1 rescues TDP-43 toxicity, we transfected these cell lines with a small interfering RNA (siRNA) against human *DBR1* or a non-targeting control siRNA (**Fig. 2d**). Neither siRNA affected TDP-43 expression in these cells (data not shown). Whereas the non-targeting siRNA had
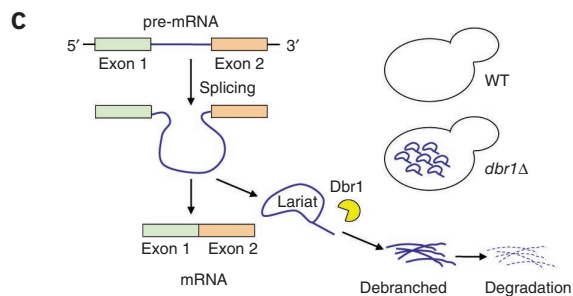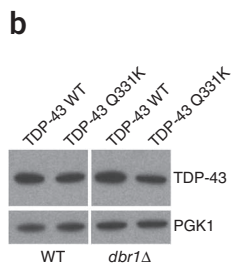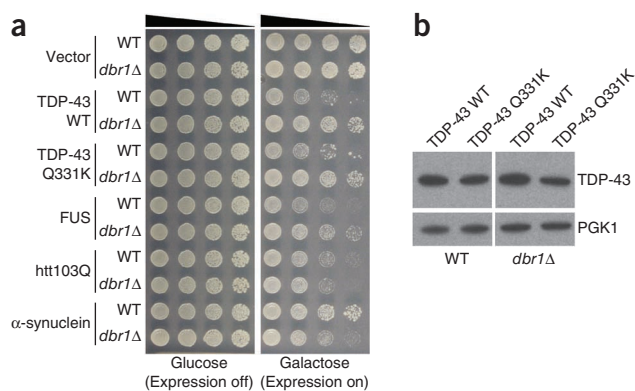
Figure 1 *DBR1* deletion suppresses TDP-43 toxicity in yeast. (**a**) Yeast spotting assays showing that *DBR1* deletion (*dbr1Δ*) suppresses TDP-43 toxicity (wild-type (WT) or ALS-linked Q331K mutant). Fivefold serial dilution of yeast cells spotted onto glucose (TDP-43 off) or galactose (TDP-43 on). (**b**) Immunoblotting shows that TDP-43 expression is not affected in *dbr1Δ* cells compared to wild-type cells. (**c**) Schematic showing the function of Dbr1 in debranching lariats following splicing. Whereas introns are rapidly degraded in wild-type cells, in *dbr1Δ* cells, intronic lariats accumulate at high levels[33].

no effect on toxicity, transfection with the *DBR1*-specific siRNA significantly reduced TDP-43 toxicity (**Fig. 2d**).

Inhibiting Dbr1 suppresses TDP-43 toxicity in primary neurons
We next asked whether knockdown of *Dbr1* prevents TDP-43 toxicity in primary neurons. We showed previously that overexpression of TDP-43 in primary cortical neurons induces neurodegeneration with cytoplasmic mislocalization and aggregation of TDP-43, recapitulating several key pathological features of TDP-43 proteinopathies *in vitro*[28]. To determine whether *Dbr1* knockdown protects neurons

from TDP-43 cytotoxicity, we used automated microscopy and longitudinal analysis, a technique that identifies and characterizes variables that significantly contribute to neuronal survival[29]. We isolated and cultured rat primary cortical neurons and transfected them with three constructs expressing (i) mApple, (ii) enhanced green fluorescent protein (EGFP) or TDP-43 fused to EGFP (TDP-43–EGFP) and (iii) siRNA directed against *Dbr1* or scrambled siRNA. With automated microscopy, hundreds of individual neurons were imaged from each cohort at regular 24-h intervals for 8 d (**Fig. 3a**). In this experiment, mApple serves as a sensitive survival marker, as the loss of mApple fluorescence, cell blebbing or disruption of the cell membrane signifies cell death[29]. These criteria are at least as specific as those used with traditional markers of particular cell death pathways but have the advantage of detecting all forms of cell death in a single assay, thereby rendering them more sensitive. Because each neuron in a population can be followed longitudinally for an extended period of time, the analysis is analogous to that used in a prospective clinical trial. Powerful statistical tools developed for human epidemiological studies, including Kaplan-Meier survival analysis and Cox proportional hazards analysis, are used to describe the data that are generated from these experiments.

We initially performed a small pilot experiment to determine the optimal amount of *Dbr1* siRNA (**Supplementary Fig. 3**) and found that the most effective dose was 30 nM. On the basis of the effect size that we noted in the pilot experiment, the population sizes of subsequent experiments were scaled to achieve the power necessary to
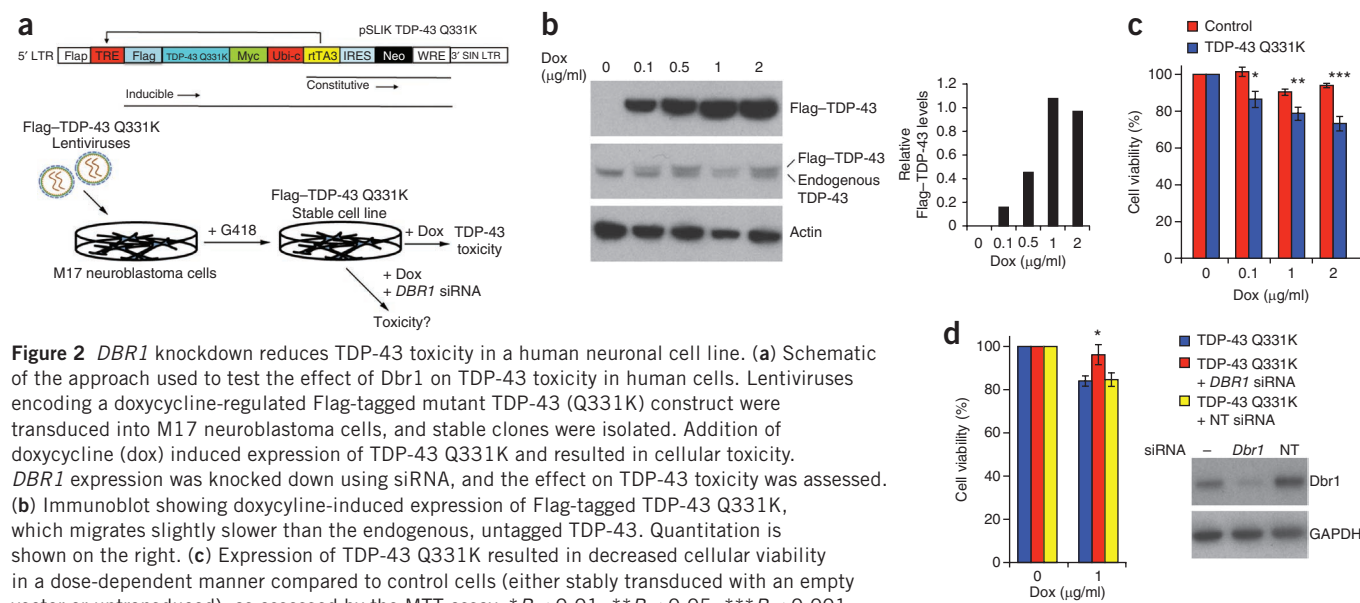

Figure 2 *DBR1* knockdown reduces TDP-43 toxicity in a human neuronal cell line. (**a**) Schematic of the approach used to test the effect of Dbr1 on TDP-43 toxicity in human cells. Lentiviruses encoding a doxycycline-regulated Flag-tagged mutant TDP-43 (Q331K) construct were transduced into M17 neuroblastoma cells, and stable clones were isolated. Addition of doxycycline (dox) induced expression of TDP-43 Q331K and resulted in cellular toxicity. *DBR1* expression was knocked down using siRNA, and the effect on TDP-43 toxicity was assessed. (**b**) Immunoblot showing doxycyline-induced expression of Flag-tagged TDP-43 Q331K, which migrates slightly slower than the endogenous, untagged TDP-43. Quantitation is shown on the right. (**c**) Expression of TDP-43 Q331K resulted in decreased cellular viability in a dose-dependent manner compared to control cells (either stably transduced with an empty vector or untransduced), as assessed by the MTT assay. $*P < 0.01$, $**P < 0.05$, $***P < 0.001$; repeated measures two-way ANOVA. Data are shown as mean ± s.e.m. (**d**) Cell viability was measured in cells transfected with an siRNA against *DBR1* or a non-targeting (NT) siRNA. The immunoblot shows effective knockdown of Dbr1 expression by the *DBR1*-specific siRNA but not the non-targeting control siRNA. $*P < 0.05$; repeated measures two-way ANOVA. Data are shown as mean ± s.e.m.

Figure 3 *Dbr1* knockdown reduces TDP-43 toxicity in primary rat neurons. (**a**) Automated fluorescence microscopy of primary rat cortical neurons transfected with constructs encoding mApple (top) and TDP-43–EGFP (bottom). Two neurons are depicted here at repeated intervals. While one of the neurons lives for the entire experiment (arrowheads), the other has died by 144 h (arrows). Scale bar, 10 μm. (**b**) Cumulative hazard plot showing the cumulative risk of death for neurons in each cohort as a function of time. Expression of TDP-43–EGFP (*n* = 380 neurons counted) significantly increases the risk of death over that of neurons expressing EGFP alone (*n* = 245 neurons counted; hazards ratio = 2.2). Knockdown of *Dbr1* using 30 nM *Dbr1* siRNA in neurons expressing TDP-43–EGFP (*n* = 300 neurons counted) decreases the risk of death by 19% compared to neurons expressing TDP-43–EGFP that received scrambled siRNA (*n* = 380 neurons counted). Data were pooled from two independent experiments, and statistical significance was determined using Cox proportional hazards analysis. ***, hazards ratio = 2.23 and $P < 1 \times 10^{-9}$; **, hazards ratio = 1.83 and $P < 1 \times 10^{-4}$; *, hazards ratio = 0.81 and $P = 0.04$. (**c**) Kaplan-Meier survival curve of the same data. (**d**) *Dbr1* knockdown results in increased percentage of neurons containing cytoplasmic TDP-43 compared to neurons treated with control, scrambled siRNA. Data are shown as mean ± s.e.m. *$P < 0.0005$, two-tailed *t* test.
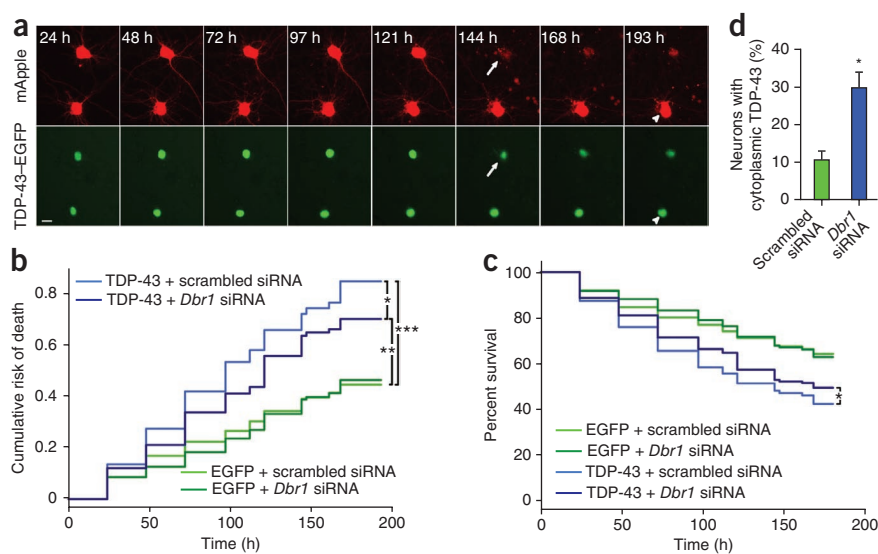
detect a significant effect on neuronal survival. As expected, the risk of death in primary cortical neurons was significantly greater in neurons expressing TDP-43–EGFP than in control neurons expressing EGFP alone (**Fig. 3b**). The relative risk or hazard ratio calculated by Cox proportional hazards analysis was 2.23 ($P < 1 \times 10^{-9}$), signifying an approximately twofold increase in the risk of death. Knockdown of *Dbr1* in neurons expressing TDP-43–EGFP reduced the risk of death by nearly 20%, with a hazards ratio of 0.81 ($P = 0.04$). In contrast, knocking down *Dbr1* had no effect on the survival of the control cohort expressing EGFP alone (hazards ratio 1.2, $P = 0.3$). Using a Kaplan-Meier survival curve to display the same data revealed a similar effect on neuron survival (**Fig. 3c**). Notably, the improvement in survival mediated by *Dbr1* knockdown did not depend on decreased amounts of cytoplasmic TDP-43. In fact, we observed significantly more primary neurons with cytoplasmic TDP-43 when treated with *Dbr1* siRNA than with control siRNA (**Fig. 3d**). These data suggest that neurons can survive even in the presence of cytoplasmic TDP-43. These results in primary neurons expressing human TDP-43 extend the protective effect of *Dbr1* knockdown that we observed in yeast and in neuroblastoma cells and indicate that the ability of Dbr1 inhibition to suppress the toxic effects of TDP-43 accumulation is conserved from yeast to mammalian cells, organisms separated by a billion years of evolutionary divergence.

Dbr1 enzymatic activity is required for TDP-43 toxicity

DBR1 encodes an RNA debranching enzyme, highly conserved from yeast to man, that cleaves the 2′–5′ phosphodiester bonds of lariat introns that are formed during pre-mRNA splicing[30,31] (**Fig. 1c**). After transcription, primary pre-mRNA transcripts are processed by the spliceosome to remove introns, which are released as lariats[32]. Lariats are formed during splicing when the 5′ exon attacks the 3′ splice site in a nucleophilic manner. RNA nucleases within the cell can digest the 3′ tail of the lariat introns, but the lariat structure is resistant to digestion until Dbr1, a specialized debranching enzyme, cleaves the 2′-hydroxyl-5′-phosphate bond (**Fig. 1c**). Debranching seems to be a rate-limiting step for the turnover of intronic RNA, as the steady-state levels of lariat introns are greatly increased in *dbr1*Δ cells[31,33].

Depletion of Dbr1 reduced TDP-43 toxicity in yeast (**Fig. 1**), mammalian cells (**Fig. 2**) and primary neurons (**Fig. 3**), but it was unclear whether the rescue was because of loss of debranching enzymatic activity or was potentially related to another Dbr1 function. To test this directly, we used 'debranching activity–dead' mutants of Dbr1. We cotransformed *dbr1*Δ yeast cells with expression plasmids for human TDP-43 and either wild-type yeast Dbr1 or two independent Dbr1 point mutants (Asp40Ala or Asn85Ala) that lack debranching enzymatic activity *in vitro* and *in vivo*[33]. Immunoblotting confirmed that the wild-type and mutant Dbr1 proteins were expressed at equivalent levels (**Fig. 4a**). Whereas expressing wild-type Dbr1 restored TDP-43 toxicity to *dbr1*Δ cells, expressing either of the debranching-inactive Dbr1 point mutants did not (**Fig. 4b**). Moreover, we tested a panel of 16 Dbr1 mutants, including some that retain full debranching activity, some that have lost all activity and some with partial debranching activity[33]. There was an exact correlation between debranching activity and the ability to restore TDP-43 toxicity to *dbr1*Δ cells: wild-type Dbr1 fully restored TDP-43 toxicity, whereas completely inactive Dbr1 had no effect, and partially active Dbr1 partially restored TDP-43 toxicity (**Supplementary Table 1**). Thus, inhibiting Dbr1 debranching enzymatic activity is sufficient to rescue TDP-43 toxicity in yeast cells. Finally, expressing mouse Dbr1 in *dbr1*Δ cells was also sufficient to restore TDP-43 toxicity (**Fig. 4b**), indicating that the debranching function of Dbr1 is conserved from yeast to mammals.

Lariat intron accumulation suppresses TDP-43 toxicity

In the absence of Dbr1, steady-state levels of lariat introns are greatly increased[33]. This suggested the intriguing possibility that the accumulating lariat introns in *dbr1*Δ cells could act as a kind of decoy for TDP-43, sequestering it away from important cellular RNAs and other RNA-binding proteins. To test this, we first determined whether the rescue of TDP-43 toxicity was specific to lariat intron accumulation or if accumulation of any nonspecific RNA species rescued toxicity. We expressed TDP-43 in three other yeast deletion strains (*upf1*Δ, *upf2*Δ and *xrn1*Δ) that each result in accumulation of RNA species within the cell, owing to alterations in the nonsense-mediated mRNA decay (NMD) pathway[34–38]. Whereas deleting *DBR1* rescued
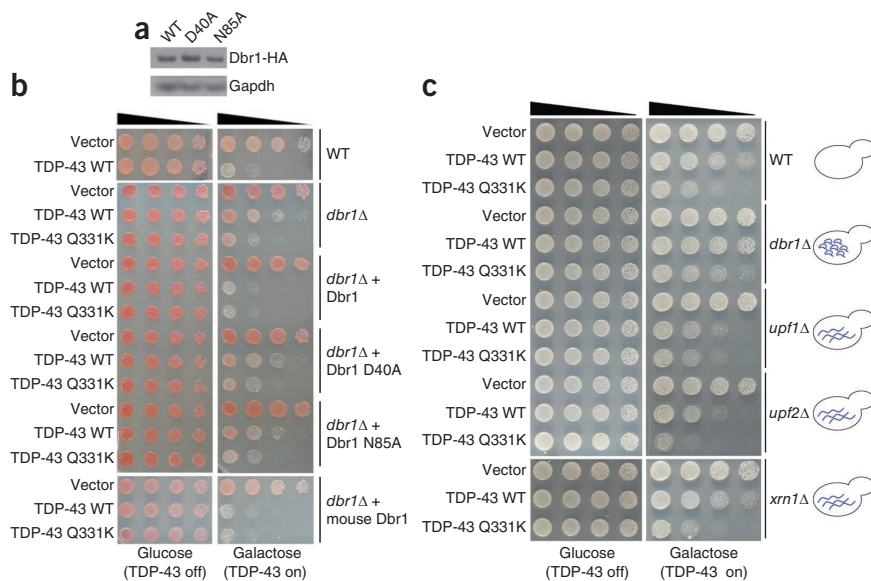
Figure 4 Dbr1 lariat debranching enzymatic activity is required for TDP-43 toxicity, and TDP-43 toxicity suppression is mediated by lariat intron accumulation. (**a**) Immunoblot showing that HA-tagged wild-type (WT) yeast Dbr1 and debranching activity–dead point mutants[33] are expressed at similar levels. (**b**) Yeast spotting assays showing that TDP-43 toxicity is suppressed in *dbr1Δ* cells. Expressing wild-type yeast Dbr1 in *dbr1Δ* cells restored toxicity. Two Dbr1 mutants (D40A and N85A) that lack debranching activity were unable to restore TDP-43 toxicity to *dbr1Δ* cells. Expressing mouse Dbr1 in *dbr1Δ* yeast cells restored TDP-43 toxicity, indicating that the function of Dbr1 is conserved from yeast to mammals. (**c**) Yeast spotting assay showing that TDP-43 toxicity is suppressed in *dbr1Δ* cells but not in three other deletion strains (*upf1Δ*, *upf2Δ* and *xrn1Δ*), which each accumulate non-specific RNA species, owing to defects in the cellular NMD pathway. Schematic of yeast cells accumulating no excess RNA species (WT), lariat RNAs (*dbr1Δ*) or nonspecific linear RNAs (*upf1Δ*, *upf2Δ* or *xrn1Δ*) are shown next to the spotting assays.

TDP-43 toxicity, TDP-43 toxicity was not suppressed in *upf1Δ*, *upf2Δ* or *xrn1Δ* cells and was even slightly enhanced in *upf1Δ* and *upf2Δ* cells (**Fig. 4c**), suggesting that the rescue of TDP-43 toxicity is specific to intronic lariat accumulation.

Intronic lariats suppress TDP-43 toxicity in the cytoplasm

We next sought to determine the mechanism by which intronic lariats suppress TDP-43 toxicity in *dbr1Δ* cells. We and others have shown that TDP-43 is toxic in the cytoplasm in multiple cellular and animal model systems[19,28,39,40]. Thus, we reasoned that intronic lariats might accumulate in the nucleus of *dbr1Δ* cells, sequester TDP-43 there and prevent it from aggregating in the cytoplasm, thereby suppressing toxicity. In this model, sequestering TDP-43 in the cytoplasm should overcome the toxicity suppression by *dbr1Δ*. To test whether this was the case, we retained TDP-43 in the cytoplasm by mutating its nuclear localization signal (NLS)[22,41]. We reasoned that, if *dbr1Δ* suppresses TDP-43 toxicity in the nucleus, the TDP-43 mutant lacking an NLS would still be toxic. Unexpectedly, *DBR1* deletion still suppressed toxicity when TDP-43 was sequestered in the cytoplasm (**Fig. 5a**), suggesting that the site of action of intronic lariats is the cytoplasm.

The above genetic result suggested that intronic lariats act in the cytoplasm to suppress TDP-43 toxicity. To test this idea directly, we developed a method to visualize in living cells the endogenous intronic lariats that accumulate in *dbr1Δ* cells. We reasoned that, if we could visualize the intronic lariats, we could determine (i) whether they localized to the cytoplasm or nucleus and (ii) whether they colocalized with TDP-43 inclusions. A technique to visualize the localization of endogenous mRNAs in living yeast cells was

recently developed[42]. m-TAG uses homologous recombination to insert binding sites for the RNA-binding MS2 coat protein (MS2-CP) between the coding region and 3′ UTR of any yeast gene. Expression of MS2-CP fused to GFP enables the visualization of any yeast mRNA that has been tagged with MS2-binding sites[42–44]. We modified m-TAG to visualize intronic lariats. Instead of tagging the 3′ UTR of a target yeast gene, we used homologous recombination to integrate MS2-binding sites in the intron of the *ACT1* gene (**Fig. 5b**), which has previously been shown by RNA blot analysis to accumulate in the absence of Dbr1 activity[33].

We transformed wild-type and *dbr1Δ* yeast cells, each harboring MS2-binding sites integrated in the intron of the *ACT1* gene (**Fig. 5c**), with a plasmid containing a 3× GFP–tagged MS2-CP RNA-binding protein under control of the inducible *MET25* promoter. We analyzed the localization of MS2-CP–GFP by fluorescence microscopy. As reported[43], because the *MET25* promoter is somewhat leaky, we detected the GFP fusion protein even without induction (by growth in the presence of methionine). In wild-type cells, in which no intronic lariats should accumulate[33], we detected faint MS2-CP–GFP expression in a diffuse pattern throughout the cell (**Fig. 5c** and **Supplementary Fig. 4**). In contrast, in *dbr1Δ* cells, MS2-CP–GFP

accumulated in one or two bright foci per cell, and these were always located in the cytoplasm (**Fig. 5c**). We observed similar results by tagging an independent intron from another yeast gene, *CYH2* (data not shown). These foci could represent the excised lariat introns that accumulate in *dbr1Δ* cells or a splicing intermediate[45] (**Supplementary Fig. 5** and **Supplementary Note**). However, as we did not see them in wild-type cells in which *ACT1* or *CYH2* introns were tagged with MS2-binding sequences (**Fig. 5c** and **Supplementary Fig. 4**), these foci are likely to be lariat introns that accumulate in the absence of Dbr1 activity.

Intronic lariats colocalize with TDP-43 cytoplasmic foci in yeast

Having established that intronic lariats accumulate in the cytoplasm of *dbr1Δ* cells, we next tested our hypothesis that the accumulating lariats in *dbr1Δ* cells act as a decoy for TDP-43 by preventing it from interacting with other important cellular RNAs and RNA-binding proteins. We expressed untagged TDP-43 in wild-type and *dbr1Δ* cells and visualized its localization by immunocytochemistry with a TDP-43–specific antibody (**Fig. 5d,e**). We visualized tagged intronic lariats by fluorescence microscopy. Notably, in every *dbr1Δ* cell analyzed, TDP-43 colocalized with intronic lariats (**Fig. 5e**). Consistent with our genetic results (**Fig. 5a**) and fluorescence microscopy experiments (**Fig. 5c**), TDP-43 was not retained in the nucleus in *dbr1Δ* cells and accumulated in the cytoplasm (**Fig. 5e**). However, the size and shape of TDP-43 inclusions were profoundly different in wild-type and *dbr1Δ* cells. In wild-type cells, TDP-43 formed multiple small, irregularly shaped cytoplasmic foci (**Fig. 5d**), whereas in *dbr1Δ* cells, TDP-43 always formed at least one large, perfectly round focus (**Fig. 5d**), which always colocalized with intronic lariats (**Fig. 5e**).
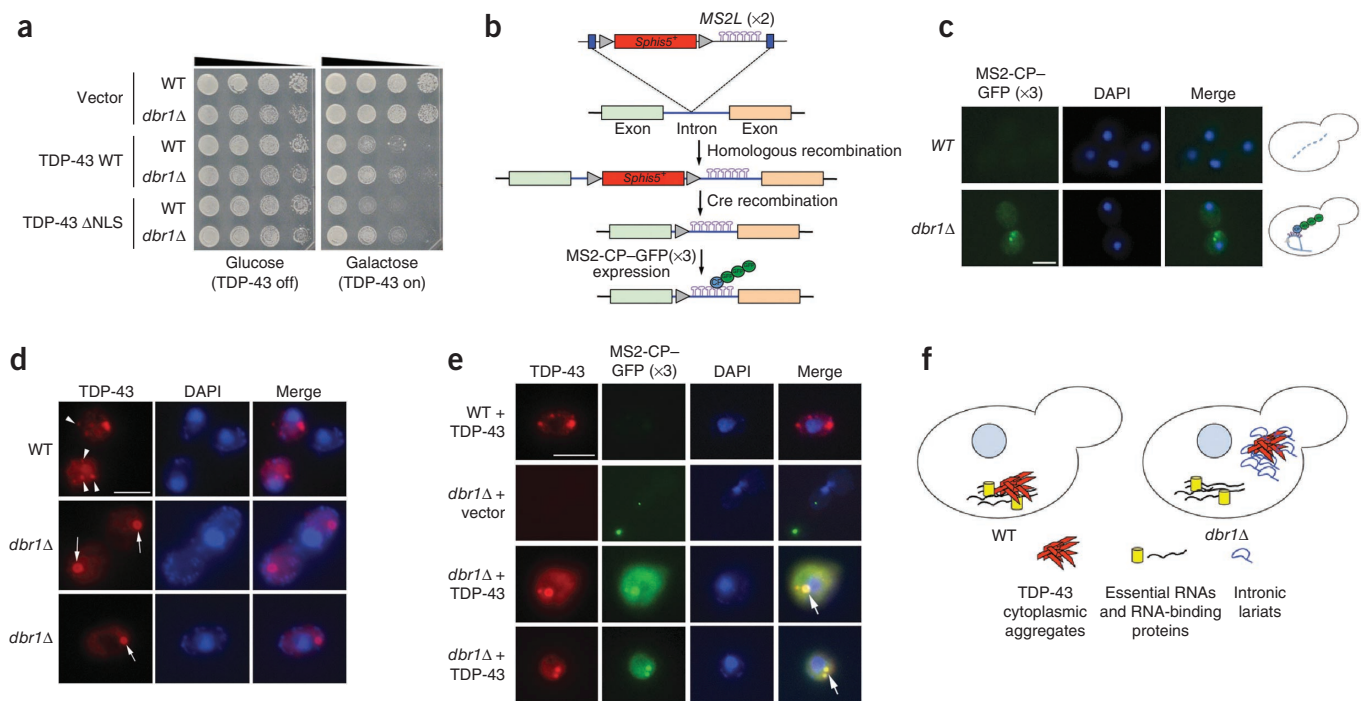
Figure 5 Intronic lariats colocalize with TDP-43 cytoplasmic foci in yeast. (**a**) The toxicity of a TDP-43 mutant that is retained in the cytoplasm (ΔNLS) is also suppressed by *dbr1Δ*. (**b**) Strategy to visualize lariat introns in living cells. Homologous recombination was used to insert an MS2 RNA-binding sequence in the intron of the *ACT1* gene. A GFP-tagged MS2-CP protein was used to visualize accumulated intronic lariats. (**c**) In wild-type cells, lariat introns did not accumulate, and the MS2-CP–GFP signal was faint and diffusely localized throughout the cell. In contrast, in *dbr1Δ* cells, MS2-CP–GFP accumulated in one or two bright foci per cell, and these were always located in the cytoplasm. Scale bar, 5 μm. (**d**) The size and shape of TDP-43 cytoplasmic inclusions were different in *dbr1Δ* cells compared to wild-type cells. Whereas in wild-type cells, TDP-43 formed multiple small, irregularly shaped foci (arrowheads), in *dbr1Δ* cells, there was always at least one large, perfectly round focus per cell (arrows). Scale bar, 5 μm. (**e**) Untagged TDP-43 was expressed in wild-type and *dbr1Δ* cells and visualized by immunocytochemistry with a TDP-43–specific antibody. TDP-43 cytoplasmic foci colocalized with tagged lariat introns (arrows). Scale bar, 5 μm. (**f**) A model of how lariat intron accumulation suppresses TDP-43 cytoplasmic toxicity. In wild-type cells, TDP-43 aggregates in the cytoplasm and could interfere, via RNA binding, with essential RNAs and RNA-binding proteins. When Dbr1 activity is inhibited (for example, in *dbr1Δ* cells), lariat introns accumulate in the cytoplasm and might act as decoys, sequestering TDP-43, thereby preventing it from interfering with important cellular RNAs.

Intronic lariats compete with RNAs for binding to TDP-43

We also assessed whether the TDP-43 ribonucleoprotein complex contains lariats. We expressed Flag-tagged TDP-43 in wild-type and *dbr1Δ* cells and immunoprecipitated TDP-43 from cell lysates with an antibody to Flag. The associated RNA was separated by two-dimensional electrophoresis. Linear RNA molecules migrate in a diagonal on two-dimensional gels, but lariat and lariat breakdown products migrate in a separate arc, owing to the reduced mobility conferred by their altered structures (**Supplementary Fig. 6a**). As expected, in wild-type and *dbr1Δ* cells, TDP-43 associated with RNA. However, in *dbr1Δ* cells, the TDP-43 ribonucleoprotein complex contained additional RNA species, consistent with intronic lariats.

Finally, to directly test our hypothesis that the intronic lariats that form in *dbr1Δ* cells act as decoys for TDP-43 by competing with it for binding to other cellular RNAs, we performed *in vitro* electrophoretic mobility shift assays. Incubation of a radioactively labeled RNA probe known to bind TDP-43 (ref. 46) with recombinant TDP-43 results in a gel shift (**Supplementary Fig. 6b,c**). We isolated total RNA from wild-type and *dbr1Δ* cells and tested the ability of these RNAs to compete for binding to TDP-43. As expected, RNAs from wild-type and *dbr1Δ* cells competed for TDP-43 binding (**Supplementary Fig. 6b**), consistent with TDP-43 binding a large number of RNA targets[47]. To specifically test the ability of intronic lariats to compete for binding to TDP-43 (to act as decoys), we treated RNAs isolated from wild-type and *dbr1Δ* cells

with RNase R, which degrades all RNAs except for branched lariats[48]. When these RNase R–treated samples were incubated with the TDP-43 binding reaction, only the RNase R–treated RNAs isolated from *dbr1Δ* cells competed TDP-43 away from its binding site (**Supplementary Fig. 6c**). Thus, *dbr1Δ* cells contain an RNase R–resistant species, likely intronic lariats, that compete for binding to TDP-43.

DISCUSSION

Using two unbiased genetic screens in yeast, we discovered Dbr1 as a potent modifier of TDP-43 toxicity. We provide evidence that, in the absence of Dbr1, intronic lariats accumulate in the cytoplasm, and we propose that these act as decoys to sequester TDP-43, preventing it from interfering with essential RNAs and RNA-binding proteins. Thus, we suggest that the debranching enzymatic activity of Dbr1 could be a novel therapeutic target to combat toxic effects from cytoplasmic TDP-43 aggregation in ALS. The additional genetic modifiers of TDP-43 toxicity uncovered from these two yeast screens (**Table 1** and **Supplementary Data**) will hopefully provide even more insight into disease mechanisms and open new avenues for therapeutic intervention.

Recent studies indicate that RNA binding is an important component of TDP-43 toxicity in cellular and animal models[19,22,49,50]. One potential mechanism of neurotoxicity is that TDP-43 aggregates in the cytoplasm, sequestering essential cellular RNAs and RNA-binding

proteins away from their normal functions. This could lead to catastrophic changes in RNA metabolism, owing to defects in the stability, splicing, transport and/or translation of essential RNAs. This effect might be more deleterious to motor neurons if motor neuron–specific transcripts were preferentially sequestered by TDP-43 or even if motor neurons were simply more sensitive to subtle alterations in any of these RNA metabolic pathways. TDP-43 loss of function likely also contributes to disease. TDP-43 is depleted from the nuclei of affected neuronal populations in individuals with ALS[8], and downregulation of TDP-43 in mouse leads to widespread dysregulation of splicing[47]. Finally, TDP-43 missense variants might act in a dominant-negative manner, interfering with the function of the wild-type protein[51,52]. These three pathogenic mechanisms (gain of toxic properties in the cytoplasm, loss of function in the nucleus and dominant-negative effects) are not mutually exclusive and likely all contribute to ALS pathogenesis.

Inhibiting Dbr1 function might overcome or prevent cytoplasmic TDP-43 (and FUS) aggregates from disrupting critical RNAs and RNA-binding proteins. We propose that the accumulated intronic lariat species in $dbr1\Delta$ cells suppress TDP-43 toxicity by acting as decoys, causing TDP-43 to bind to them rather than to important cellular RNA targets (**Fig. 5f**). The catalog of genome-wide RNA targets for TDP-43 is emerging[47,53–55]. Notably, TDP-43 seems to preferentially bind to long intronic pre-mRNA sites rather than coding exonic regions or UTRs[47]. This might explain why the intronic RNA sequences (lariats) that accumulate in $dbr1\Delta$ cells sequester TDP-43 away from other RNA species in the cell and suppress TDP-43 toxicity. TDP-43 might also preferentially recognize the lariat branch-point structure, or binding to the lariat might promote nucleation or other alterations to TDP-43 conformation.

For Dbr1 to be a therapeutic target, several questions must be addressed. First, could inhibition of Dbr1 debranching activity be toxic itself? Indeed, the highest concentration of $Dbr1$ siRNA (50 nM) in primary rat neurons increased the risk of death (**Supplementary Fig. 3**), suggesting that too much Dbr1 inhibition could be deleterious. However, in budding yeast, $DBR1$ deletion is tolerated (**Fig. 1a**), and siRNA knockdown in M17 cells does not result in growth inhibition (ref. 56 and M.A. and A.D.G., unpublished data). Nevertheless, it will be important to determine what level of Dbr1 inhibition is tolerated and whether an appropriate therapeutic index can be achieved. An additional consideration for this approach in mammalian cells is the non-coding RNAs in intronic regions that depend on Dbr1 activity. Expression of these non-coding RNAs might be dysregulated by Dbr1 inhibition, and the consequences of this must be assessed. Furthermore, as abnormal accumulation of RNA is hypothesized to trigger autoimmunity and there would likely be a large pool of lariats in human cells, the effects of Dbr1 inhibition on autoimmunity should be analyzed. Although, to our knowledge, Dbr1 inhibitors are not available, our new method to visualize intronic lariats in living cells (**Fig. 4**) will facilitate screening of chemical compound libraries for small molecule Dbr1 inhibitors.

There are currently no TDP-43–directed therapies for ALS or related TDP-43 proteinopathies. Antisense oligonucleotides and RNA interference approaches are emerging as attractive therapeutic strategies in neurodegenerative diseases in which decreasing levels of a toxic mutant protein might be efficacious[57–60]. Indeed, treating a mouse model of inherited ALS (caused by a mutation in $SOD1$) with antisense oligonucleotides to $SOD1$ significantly slowed disease progression[4]. This approach offers tremendous promise for treating patients with ALS with $SOD1$ mutations, but, as mutations in $SOD1$ account for only ~2–5% of all ALS cases, additional therapeutic strategies are needed. Because TDP-43 appears to contribute to ALS pathogenesis broadly[7], targeting TDP-43 with antisense approaches could be effective. However, it is unknown whether TDP-43 contributes to disease via loss- or gain-of-function mechanisms[61], mandating caution in pursuing TDP-43–lowering approaches. We present an alternative strategy: by targeting Dbr1 using small molecule inhibitors or antisense oligonucleotides, it might be possible to antagonize the toxic effects of TDP-43 in the cytoplasm without interfering with potentially critical functions in the nucleus.

URLs. Study protocols, http://www.gladstone.ucsf.edu/gladstone/site/finkbeiner/.

METHODS
Methods and any associated references are available in the online version of the paper.

Note: Supplementary information is available in the online version of the paper.

AUTHOR CONTRIBUTIONS
M.A., M.J.H., M.D.F., S.J.B., J.S., N.J.K., S.F., R.V.F. and A.D.G. designed the experiments. M.A., M.J.H., M.D.F., S.J.B., J.S., E.A.S., Z.D., X.F. and A.D.G. performed the research. M.A., M.J.H., M.D.F., S.J.B., J.S., N.J.K., S.F., R.V.F. and A.D.G. analyzed and interpreted data. M.A., M.J.H., M.D.F., S.J.B., S.F., R.V.F. and A.D.G. wrote the manuscript with contributions from all authors.

1. Boillée, S., Vande Velde, C. & Cleveland, D.W. ALS: a disease of motor neurons and their nonneuronal neighbors. *Neuron* **52**, 39–59 (2006).
2. Rosen, D.R. *et al.* Mutations in Cu/Zn superoxide dismutase gene are associated with familial amyotrophic lateral sclerosis. *Nature* **362**, 59–62 (1993).

3. Bruijn, L.I. *et al.* Aggregation and motor neuron toxicity of an ALS-linked SOD1 mutant independent from wild-type SOD1. *Science* **281**, 1851–1854 (1998).

4. Smith, R.A. *et al.* Antisense oligonucleotide therapy for neurodegenerative disease. *J. Clin. Invest.* **116**, 2290–2296 (2006).

5. Lagier-Tourenne, C., Polymenidou, M. & Cleveland, D.W. TDP-43 and FUS/TLS: emerging roles in RNA processing and neurodegeneration. *Hum. Mol. Genet.* **19**, R46–R64 (2010).

6. Gitler, A.D. & Shorter, J. RNA-binding proteins with prion-like domains in ALS and FTLD-U. *Prion* **5**, 179–187 (2011).

7. Mackenzie, I.R. *et al.* Pathological TDP-43 distinguishes sporadic amyotrophic lateral sclerosis from amyotrophic lateral sclerosis with *SOD1* mutations. *Ann. Neurol.* **61**, 427–434 (2007).

8. Neumann, M. *et al.* Ubiquitinated TDP-43 in frontotemporal lobar degeneration and amyotrophic lateral sclerosis. *Science* **314**, 130–133 (2006).

9. Pesiridis, G.S., Lee, V.M. & Trojanowski, J.Q. Mutations in TDP-43 link glycine-rich domain functions to amyotrophic lateral sclerosis. *Hum. Mol. Genet.* **18**, R156–R162 (2009).

10. Rutherford, N.J. *et al.* Novel mutations in *TARDBP* (TDP-43) in patients with familial amyotrophic lateral sclerosis. *PLoS Genet.* **4**, e1000193 (2008).

11. Sreedharan, J. *et al.* TDP-43 mutations in familial and sporadic amyotrophic lateral sclerosis. *Science* **319**, 1668–1672 (2008).

12. Van Deerlin, V.M. *et al.* *TARDBP* mutations in amyotrophic lateral sclerosis with TDP-43 neuropathology: a genetic and histopathological analysis. *Lancet Neurol.* **7**, 409–416 (2008).

13. Yokoseki, A. *et al.* TDP-43 mutation in familial amyotrophic lateral sclerosis. *Ann. Neurol.* **63**, 538–542 (2008).

14. Belzil, V.V. *et al.* Mutations in *FUS* cause FALS and SALS in French and French Canadian populations. *Neurology* **73**, 1176–1179 (2009).

15. Corrado, L. *et al.* Mutations of *FUS* gene in sporadic amyotrophic lateral sclerosis. *J. Med. Genet.* **47**, 190–194 (2010).

16. Hewitt, C. *et al.* Novel *FUS/TLS* mutations and pathology in familial and sporadic amyotrophic lateral sclerosis. *Arch. Neurol.* **67**, 455–461 (2010).

17. Kwiatkowski, T.J. Jr. *et al.* Mutations in the *FUS/TLS* gene on chromosome 16 cause familial amyotrophic lateral sclerosis. *Science* **323**, 1205–1208 (2009).

18. Vance, C. *et al.* Mutations in FUS, an RNA processing protein, cause familial amyotrophic lateral sclerosis type 6. *Science* **323**, 1208–1211 (2009).

19. Johnson, B.S., McCaffery, J.M., Lindquist, S. & Gitler, A.D. A yeast TDP-43 proteinopathy model: exploring the molecular determinants of TDP-43 aggregation and cellular toxicity. *Proc. Natl. Acad. Sci. USA* **105**, 6439–6444 (2008).

20. Johnson, B.S. *et al.* TDP-43 is intrinsically aggregation-prone, and amyotrophic lateral sclerosis–linked mutations accelerate aggregation and increase toxicity. *J. Biol. Chem.* **284**, 20329–20339 (2009).

21. Sun, Z. *et al.* Molecular determinants and genetic modifiers of aggregation and toxicity for the ALS disease protein FUS/TLS. *PLoS Biol.* **9**, e1000614 (2011).

22. Elden, A.C. *et al.* Ataxin-2 intermediate-length polyglutamine expansions are associated with increased risk for ALS. *Nature* **466**, 1069–1075 (2010).

23. Lagier-Tourenne, C. & Cleveland, D.W. Neurodegeneration: an expansion in ALS genetics. *Nature* **466**, 1052–1053 (2010).

24. Willingham, S., Outeiro, T.F., DeVit, M.J., Lindquist, S.L. & Muchowski, P.J. Yeast genes that enhance the toxicity of a mutant huntingtin fragment or α-synuclein. *Science* **302**, 1769–1772 (2003).

25. Giorgini, F., Guidetti, P., Nguyen, Q., Bennett, S.C. & Muchowski, P.J. A genomic screen in yeast implicates kynurenine 3-monooxygenase as a therapeutic target for Huntington disease. *Nat. Genet.* **37**, 526–531 (2005).

26. Tong, A.H. *et al.* Systematic genetic analysis with ordered arrays of yeast deletion mutants. *Science* **294**, 2364–2368 (2001).

27. Schuldiner, M. *et al.* Exploration of the function and organization of the yeast early secretory pathway through an epistatic miniarray profile. *Cell* **123**, 507–519 (2005).

28. Barmada, S.J. *et al.* Cytoplasmic mislocalization of TDP-43 is toxic to neurons and enhanced by a mutation associated with familial amyotrophic lateral sclerosis. *J. Neurosci.* **30**, 639–649 (2010).

29. Arrasate, M., Mitra, S., Schweitzer, E.S., Segal, M.R. & Finkbeiner, S. Inclusion body formation reduces levels of mutant huntingtin and the risk of neuronal death. *Nature* **431**, 805–810 (2004).

30. Arenas, J. & Hurwitz, J. Purification of a RNA debranching activity from HeLa cells. *J. Biol. Chem.* **262**, 4274–4279 (1987).

31. Chapman, K.B. & Boeke, J.D. Isolation and characterization of the gene encoding yeast debranching enzyme. *Cell* **65**, 483–492 (1991).

32. Domdey, H. *et al.* Lariat structures are *in vivo* intermediates in yeast pre-mRNA splicing. *Cell* **39**, 611–621 (1984).

33. Khalid, M.F., Damha, M.J., Shuman, S. & Schwer, B. Structure-function analysis of yeast RNA debranching enzyme (Dbr1), a manganese-dependent phosphodiesterase. *Nucleic Acids Res.* **33**, 6349–6360 (2005).

34. Franks, T.M., Singh, G. & Lykke-Andersen, J. Upf1 ATPase-dependent mRNP disassembly is required for completion of nonsense-mediated mRNA decay. *Cell* **143**, 938–950 (2010).

35. Gatfield, D. & Izaurralde, E. Nonsense-mediated messenger RNA decay is initiated by endonucleolytic cleavage in *Drosophila*. *Nature* **429**, 575–578 (2004).

36. Lejeune, F., Li, X. & Maquat, L.E. Nonsense-mediated mRNA decay in mammalian cells involves decapping, deadenylating, and exonucleolytic activities. *Mol. Cell* **12**, 675–687 (2003).

37. Larimer, F.W., Hsu, C.L., Maupin, M.K. & Stevens, A. Characterization of the *XRN1* gene encoding a 5′→3′ exoribonuclease: sequence data and analysis of disparate protein and mRNA levels of gene-disrupted yeast cells. *Gene* **120**, 51–57 (1992).

38. van Dijk, E.L. *et al.* XUTs are a class of Xrn1-sensitive antisense regulatory non-coding RNA in yeast. *Nature* **475**, 114–117 (2011).

39. Igaz, L.M. *et al.* Dysregulation of the ALS-associated gene TDP-43 leads to neuronal death and degeneration in mice. *J. Clin. Invest.* **121**, 726–738 (2011).

40. Zhang, Y.J. *et al.* Aberrant cleavage of TDP-43 enhances aggregation and cellular toxicity. *Proc. Natl. Acad. Sci. USA* **106**, 7607–7612 (2009).

41. Winton, M.J. *et al.* Disturbance of nuclear and cytoplasmic TAR DNA-binding protein (TDP-43) induces disease-like redistribution, sequestration, and aggregate formation. *J. Biol. Chem.* **283**, 13302–13309 (2008).

42. Haim, L., Zipor, G., Aronov, S. & Gerst, J.E. A genomic integration method to visualize localization of endogenous mRNAs in living yeast. *Nat. Methods* **4**, 409–412 (2007).

43. Haim-Vilmovsky, L. & Gerst, J.E. m-TAG: a PCR-based genomic integration method to visualize the localization of specific endogenous mRNAs *in vivo* in yeast. *Nat. Protoc.* **4**, 1274–1284 (2009).

44. Haim-Vilmovsky, L. & Gerst, J.E. Visualizing endogenous mRNAs in living yeast using m-TAG, a PCR-based RNA aptamer integration method, and fluorescence microscopy. *Methods Mol. Biol.* **714**, 237–247 (2011).

45. Mayas, R.M., Maita, H., Semlow, D.R. & Staley, J.P. Spliceosome discards intermediates via the DEAH box ATPase Prp43p. *Proc. Natl. Acad. Sci. USA* **107**, 10020–10025 (2010).

46. Buratti, E. & Baralle, F.E. Characterization and functional implications of the RNA binding properties of nuclear factor TDP-43, a novel splicing regulator of *CFTR* exon 9. *J. Biol. Chem.* **276**, 36337–36343 (2001).

47. Polymenidou, M. *et al.* Long pre-mRNA depletion and RNA missplicing contribute to neuronal vulnerability from loss of TDP-43. *Nat. Neurosci.* **14**, 459–468 (2011).

48. Suzuki, H. *et al.* Characterization of RNase R–digested cellular RNA source that consists of lariat and circular RNAs from pre-mRNA splicing. *Nucleic Acids Res.* **34**, e63 (2006).

49. Voigt, A. *et al.* TDP-43–mediated neuron loss *in vivo* requires RNA-binding activity. *PLoS ONE* **5**, e12247 (2010).

50. Li, Y. *et al.* A *Drosophila* model for TDP-43 proteinopathy. *Proc. Natl. Acad. Sci. USA* **107**, 3169–3174 (2010).

51. Yang, C. *et al.* The C-terminal TDP-43 fragments have a high aggregation propensity and harm neurons by a dominant-negative mechanism. *PLoS ONE* **5**, e15878 (2010).

52. Estes, P.S. *et al.* Wild-type and A315T mutant TDP-43 exert differential neurotoxicity in a *Drosophila* model of ALS. *Hum. Mol. Genet.* **20**, 2308–2321 (2011).

53. Sephton, C.F. *et al.* Identification of neuronal RNA targets of TDP-43–containing ribonucleoprotein complexes. *J. Biol. Chem.* **286**, 1204–1215 (2011).

54. Tollervey, J.R. *et al.* Characterizing the RNA targets and position-dependent splicing regulation by TDP-43. *Nat. Neurosci.* **14**, 452–458 (2011).

55. Xiao, S. *et al.* RNA targets of TDP-43 identified by UV-CLIP are deregulated in ALS. *Mol. Cell Neurosci.* **47**, 167–180 (2011).

56. Ye, Y., De Leon, J., Yokoyama, N., Naidu, Y. & Camerini, D. *DBR1* siRNA inhibition of HIV-1 replication. *Retrovirology* **2**, 63 (2005).

57. Xia, H., Mao, Q., Paulson, H.L. & Davidson, B.L. siRNA-mediated gene silencing *in vitro* and *in vivo*. *Nat. Biotechnol.* **20**, 1006–1010 (2002).

58. Xia, H. *et al.* RNAi suppresses polyglutamine-induced neurodegeneration in a model of spinocerebellar ataxia. *Nat. Med.* **10**, 816–820 (2004).

59. Singer, O. *et al.* Targeting *BACE1* with siRNAs ameliorates Alzheimer disease neuropathology in a transgenic model. *Nat. Neurosci.* **8**, 1343–1349 (2005).

60. Kordasiewicz, H.B. *et al.* Sustained therapeutic reversal of Huntington's disease by transient repression of Huntingtin synthesis. *Neuron* **74**, 1031–1044 (2012).

61. Da Cruz, S. & Cleveland, D.W. Understanding the role of TDP-43 and FUS/TLS in ALS and beyond. *Curr. Opin. Neurobiol.* **21**, 904–919 (2011).

ONLINE METHODS

Yeast strains, media and plasmids. The *dbr1Δ* strain was obtained by replacing the *DBR1* coding region with a KanMX4 cassette in the BY4741 or W303 strain and verified by colony PCR. CEN and 2-micron galactose-inducible TDP-43 (ref. 28), 2-micron ΔNLS-TDP-43-YFP[22], FUS[21], α-synuclein[62] and Htt103Q expression plasmids were as described[63]. The yeast Dbr1 mutant expression plasmids[33] and m-TAG plasmids pLOXHIS5MS2L, pSH47 and pMS2-CP-GFP (×3) were as described[44].

Yeast TDP-43 toxicity modifier screens. We used the SGA technique to screen the collection of nonessential-only yeast knockout strains (screen 1, performed in the laboratory of A.D.G.) or a collection of nonessential yeast knockout strains combined with essential genes reduced in expression by DAmP[27] (screen 2, performed in the laboratories of R.V.F. and N.K.) for modifiers of TDP-43 toxicity. These screens were performed as described[26,64,65], with some modifications[66], using a Singer RoToR HDA (Singer Instruments). For screen 1, the galactose-inducible TDP-43 expression construct (pAG416Gal–TDP-43) was introduced into MATα strain Y7092 to generate the query strain. This query strain was mated to the yeast haploid deletion collection of nonessential genes (MATα, each gene deleted by KanMX cassette; **Fig. 1a**). Haploid mutants harboring the TDP-43 expression plasmid were grown in the presence of glucose (TDP-43 expression off) or galactose (TDP-43 expression on). After growth at 30 °C for 2 d, plates were photographed, and colony sizes were measured by ImageJ image analysis software as described[67]. The entire screen was repeated three times, and only hits that were reproduced all three times were selected for further validation by random spore analysis on DNA sequencing of deletion strain barcodes.

For screen 2, a control query strain containing the empty vector was generated by transforming the yeast strain BY5563 (Matα) with p415-Gal-GFP, and the experimental query strain was generated by transforming BY5563 (Matα) with p415-Gal–TDP-43–GFP. Both strains were mated with the combined yeast knockout DAmP collection (Matα). Haploid yeast containing the deletion/DAmP yeast gene with the control or experiment plasmid were selected as described[65]. Three biological replicates were isolated by selecting for haploid yeast after sporulation on three plates. Each biological replicate was duplicated to generate six replicates (three biological and two technical replicates per biological replicate). Plates were imaged at several time points after final inoculation on glucose or galactose. Colony size was assessed as described[67].

Isolation and culturing of primary cortical neurons. Rat cortical neurons were isolated from embryonic day 20–21 rat (Sprague Dawley) pups, cultured in serum-free medium in 96-well plates for 4 d *in vitro* and then transfected using Lipofectamine 2000 (Invitrogen; see URLs for full protocols). Neurons were transfected with plasmids (pGW1 backbone) encoding mApple and either TDP-43–EGFP or EGFP and with siRNA directed against *Dbr1* (SMARTpool, Dharmacon) or scrambled siRNA (Dharmacon).

Live-cell imaging for longitudinal analysis. For neuronal survival analysis, we used a robotic imaging system as described[68,69]. Briefly, approximately 24–48 h after transfection, images were acquired with an inverted Nikon microscope (TE2000) equipped with PerfectFocus, an extra-long working distance (ELWD) 20× objective lens and an Andor Clara 16-bit, ultra-cooled camera. Illumination was provided by an adjustable, high-intensity and long-lasting xenon lamp, and a liquid light guide was used to maximize the signal-to-noise ratio. The stage and shutter movements, fluorescence excitation and emission filters, focusing and image acquisition were fully automated and were controlled through a 64-bit host computer running a combination of proprietary software (ImagePro, Media Cybernetics) and custom-designed algorithms.

Survival analysis. Digitized images from the red fluorescent protein (RFP; mApple) and green fluorescent protein (GFP; TDP-43–EGFP) channels were assembled into montages with ImagePro, and cells were prospectively counted in the RFP channel by original code developed in Matlab. Cell death was marked by loss of fluorescence, membrane rupture or neurite retraction. The time of death for each neuron was defined as the last time the neuron was seen. Kaplan-Meier and cumulative risk of death curves were generated using the

survival package in R. Statistical significance of survival differences between cohorts of neurons was determined by the log-rank test, and Cox proportional hazards analysis was used to measure the relative change in the risk of death, the hazard ratio.

Two-dimensional nucleic acid gels. Nucleic acid pellets from immunoprecipitation were resuspended in 5 μl of nuclease-free water and 5 μl of 2× nucleic acid loading dye (0.025 g xylene cyanol and 0.025 g bromophenol blue in 100% formamide) and were heated at 85 °C for 5 min. Nucleic acids were separated in the first dimension by loading samples into a prerun (300 V for 10 min) 5% polyacrylamide gel (19:1 acrylamide:bis-acrylamide) containing 7 M urea and 1× TBE (90 mM Tris base, 90 mM boric acid, 2 mM EDTA, pH 8.0) and electrophoresing them at 300 V. Nucleic acids were separated in the second dimension by placing the entire lane from the first-dimension gel above the second-dimension gel. The second-dimension gel was exactly the same as the first-dimension gel, except that it contained 10% polyacrylamide. Samples were electrophoresed at 300 V until xylene cyanol dye reached the bottom of the second-dimension gel. Two-dimensional nucleic acid gels were washed briefly in water and then placed in 1× SYBR Gold (Invitrogen) solution prepared in water. Gels were protected from light and gently agitated at 23–25 °C in 1× SYBR Gold solution for 45 min. Images of the gels were captured on an ultraviolet light box at an excitation wavelength of 302 nm with a 4-s exposure time.

Genomic tagging strategy to visualize intronic lariats. To visualize intronic lariats in *dbr1Δ* cells, we adapted the m-TAG protocol[42] for use with introns. We used PCR-based chromosomal gene tagging, using homologous recombination to integrate the *loxP∷Sphis5⁺∷loxP∷MS2L* cassette into the intron of either the *ACT1* gene or the *CYH2* gene in wild-type or *dbr1Δ* cells. For *ACT1*, we inserted the *MS2L* cassette at nucleotide 159 of the *ACT1* genomic DNA sequence (ACT1/YFL039C on chromosome VI from coordinates 54,696 to 53,260). For *CYH2*, we inserted the *MS2L* cassette at nucleotide 303 of the *CYH2* genomic DNA sequence (RPL28/YGL103W on chromosome VII from coordinates 310,967 to 311,927). To excise the *loxP*-flanked *Sphis5* cassette, we transformed cells with plasmid pSH47, which expresses Cre recombinase under control of a galactose-regulated promoter. Proper integration of *MS2L* sequences was verified by colony PCR and DNA sequencing.

Visualizing tagged intronic lariats by fluorescence microscopy. We visualized *MS2L*-tagged intronic lariats in wild-type and *dbr1Δ* cells as described[42]. We transformed wild-type and *dbr1Δ* cells harboring an *MS2L*-tagged *ACT1* intron with pMS2–CP-GFP(×3), which expresses MS2-CP fused to three copies of GFP under the control of the *MET25* promoter. Yeast cells were fixed with 70% ethanol and stained with DAPI in Vectashield mounting medium. Colocalization of an *MS2L*-tagged intronic lariat with TDP-43 was determined using fluorescence microscopy to detect lariats (GFP) and immunocytochemistry with a TDP-43–specific antibody to detect untagged TDP-43.

TDP-43 lentiviruses. To generate a lentiviral vector for the conditional expression of TDP-43 Gln331Lys, a Gateway entry clone encoding N-terminally Flag-tagged and C-terminally Myc-tagged TDP-43 Gln331Lys was used in a Gateway LR reaction (Invitrogen) to transfer it to the pSLIK-Neo lentiviral destination vector. Recombinant lentiviruses were produced as described[70]. For lentiviral transduction, human M17 neuroblastoma cells (ATCC) were incubated with lentiviral supernatants for 6 h at 37 °C. Stable cell lines were selected by culturing transduced cells for 5 d in growth medium (minimum essential medium (MEM) alpha/F-12 (Invitrogen) supplemented with 10% heat-inactivated FBS, 100 U/ml penicillin and 100 μg/ml streptomycin (complete medium) with 100 μg/ml Geneticin). Individual clones were selected and analyzed for inducible expression by immunoblotting and immunofluorescence analyses.

TDP-43 toxicity assays in mammalian cells. We assessed the effect of TDP-43 on cell proliferation in the MTT assay. M17 cells stably transduced with either an empty vector or with the vector encoding TDP-43 Gln331Lys were seeded in 96-well plates. To induce TDP-43 Gln331Lys expression, doxycycline (0.1, 1 or 2 μg/ml) was added to the growth medium, and cells were incubated

for 3 d. To measure proliferation, MTT (3-(4,5-dimethylthiazol-2-yl)-2,5-diphenyltetrazolium bromide) was added to each well, and cells were incubated for 4 h at 37 °C. Acidic isopropanol (40 mM HCl) was then added to each well to solubilize the blue formazan crystals. Absorbance at 570 nm was read with a Tecan Safire II plate reader. Absorbance measurements were normalized to the absorbance of cells not treated with doxycycline and used to calculate the percent viability under each condition. Two-way ANOVA was used to evaluate differences in means between two groups, and P values of <0.05 were considered statistically significant. Each condition was replicated at least four times, and each experiment was independently repeated at least three times.

siRNA knockdown of *DBR1* in M17 cells. siRNA targeting human *DBR1* and non-targeting control siRNA were purchased from Thermo-Scientific (*DBR1*, J-008290-08-0005; non-targeting, D-001810-01-05). siRNA knockdown was validated by immunoblotting with a Dbr1-specific antibody (Proteintech, rabbit polyclonal antibody, 16019-1-AP). The M17 cell line with inducible TDP-43 Gln331Lys expression was transfected with 50 nM human *DBR1* siRNA or non-targeting control siRNA using RNAi Lipofectamine (Invitrogen). After 2 d, cells were transferred to medium containing doxycycline (0 and 1 µg/ml) to induce expression of TDP-43, and toxicity was then assessed by MTT assay after 2 d (on day 4 after transfection). TDP-43 toxicity in M17 cells transfected with *DBR1* siRNA was compared to toxicity in cells transfected with non-targeting control siRNA or empty vector.

TDP-43 *in vitro* RNA-binding assay. Glutathione S-transferase (GST)–TDP-43 was purified from *Escherichia coli* as described[20]. RNA binding assays were performed as described[71]. Briefly, competitor RNA was purified from wild-type or *dbr1*Δ W303 yeast using the RNeasy Mini kit (Qiagen) and was either left untreated or was treated with RNase R to degrade any linear RNA structures while leaving lariat RNA intact. After RNase R treatment, RNA was purified using the RNeasy MinElute Cleanup kit (Qiagen). A radioactively labeled RNA probe, UG$_6$, which is known to bind TDP-43 (ref. 46), was generated by T7 polymerase–catalyzed transcription of a DNA template in the presence of [^{32}P]-labeled UTP. Standard binding reactions were carried out in a 10-µl volume containing 4 mM MgCl$_2$, 25 mM phosphocreatine, 1.25 mM ATP, 1.3% polyvinyl alcohol, 25 ng of yeast tRNA, 0.8 mg of BSA, 1 mM DTT, 0.1 µl Rnasin (Promega, 40 U/ml), 75 mM KCl, 10 mM Tris, pH 7.5, 0.1 mM EDTA and 10% glycerol. Binding reactions containing GST–TDP-43 (0.5 µM) and [^{32}P]-labeled UG$_6$ (1 µl) were incubated for 15 min at 30 °C in the presence of various dilutions of competitor RNA (0–12.9 µg). Binding reactions were then transferred to ice, and heparin was added to a final concentration of 0.5 µg/µl. Reactions were analyzed on a 4.5% native gel (acrylamide:bis-acrylamide (29:1), Bio-Rad).

62. Cooper, A.A. *et al.* Alpha-synuclein blocks ER-Golgi traffic and Rab1 rescues neuron loss in Parkinson's models. *Science* **313**, 324–328 (2006).
63. Duennwald, M.L. & Lindquist, S. Impaired ERAD and ER stress are early and specific events in polyglutamine toxicity. *Genes Dev.* **22**, 3308–3319 (2008).
64. Tong, A.H. *et al.* Global mapping of the yeast genetic interaction network. *Science* **303**, 808–813 (2004).
65. Tong, A.H. & Boone, C. Synthetic genetic array analysis in *Saccharomyces cerevisiae*. *Methods Mol. Biol.* **313**, 171–192 (2006).
66. Armakola, M., Hart, M.P. & Gitler, A.D. TDP-43 toxicity in yeast. *Methods* **53**, 238–245 (2011).
67. Collins, S.R., Schuldiner, M., Krogan, N.J. & Weissman, J.S. A strategy for extracting and analyzing large-scale quantitative epistatic interaction data. *Genome Biol.* **7**, R63 (2006).
68. Sharma, P., Ando, D.M., Daub, A., Kaye, J.A. & Finkbeiner, S. High-throughput screening in primary neurons. *Methods Enzymol.* **506**, 331–360 (2012).
69. Arrasate, M. & Finkbeiner, S. Automated microscope system for determining factors that predict neuronal fate. *Proc. Natl. Acad. Sci. USA* **102**, 3840–3845 (2005).
70. Shinbo, Y. *et al.* Proper SUMO-1 conjugation is essential to DJ-1 to exert its full activities. *Cell Death Differ.* **13**, 96–108 (2006).
71. Rothrock, C.R., House, A.E. & Lynch, K.W. HnRNP L represses exon splicing via a regulated exonic splicing silencer. *EMBO J.* **24**, 2792–2802 (2005).